Energy & Environmental Science

Cite this: *Energy Environ. Sci.*, 2012, **5**, 7582

www.rsc.org/ees

PAPER

Resistance and polarization losses in aqueous buffer–membrane electrolytes for water-splitting photoelectrochemical cells†

Emil A. Hernández-Pagán,[a] Nella M. Vargas-Barbosa,[a] TsingHai Wang,[a] Yixin Zhao,[a] Eugene S. Smotkin[b] and Thomas E. Mallouk*[a]

Received 9th December 2011, Accepted 2nd April 2012
DOI: 10.1039/c2ee03422k

The recent development of inexpensive catalysts for the oxygen evolution reaction has suggested that efficient photoelectrochemical cells (PECs) might be constructed from terrestrially abundant materials. Because these catalysts operate in aqueous buffer solutions at neutral to slightly basic pH, it is important to consider whether electrolytic cells can have low series loss under these conditions. Water-splitting or fuel-forming PECs will likely require porous separators or electrolyte membranes to separate the cathode products from oxygen produced at the anode. For this reason we analyze the individual potential losses in electrolytic systems of buffer solutions and commercially available anion- and cation-exchange membranes. Potentiometric analysis and pH measurements were employed to measure the potential losses associated with solution resistance, membrane resistance, and pH gradient formation at the current density (25 mA cm^{-2}) expected for efficient PECs. The membrane pH gradient is the most problematic source of loss in these systems, but monoprotic buffers can minimize the pH gradient by diffusion of the neutral acidic or basic form of the buffer across the membrane. These results suggest that water-splitting PECs can be viable with properly chosen membrane–buffer combinations.

1. Introduction

The growing energy needs of the world present a compelling challenge to develop cost-competitive alternatives to fossil fuels.[1] Renewable, carbon-neutral energy sources will be needed on the scale of terawatts to minimize the environmental consequences of increasing energy use. Hydrogen, which can be made from many different energy sources, is one of the most promising energy carriers for transportation applications. Hydrogen has a high energy density and can be used directly in fuel cells or internal combustion engines. It can also be used to reduce CO_2 catalytically to liquid fuels.

Among the different methods for producing H_2, water electrolysis has the advantage of generating pure H_2 without the need for purification. Water electrolysis can be powered by several carbon-neutral energy sources including photovoltaic (PV)-coupled electrolyzers.[2,3] In these systems, PV modules provide

[a]*Department of Chemistry, The Pennsylvania State University, University Park, Pennsylvania, 16802, USA. E-mail: tem5@psu.edu; Fax: +1 814-865-2927; Tel: +1 814-863-9637*
[b]*Department of Chemistry and Chemical Biology, Northeastern University, Boston, MA 02115, USA. E-mail: esmotkin@gmail.com*
† Electronic supplementary information (ESI) available. See DOI: 10.1039/c2ee03422k

Broader context

Solar cells that directly generate fuel from renewable feedstocks (water or carbon dioxide) are usually envisioned as two-electrode electrolysis cells in which fuel is produced at the cathode and oxygen is evolved at the anode. Recently, it has been proposed that such cells could employ inexpensive electrocatalysts that operate near neutral pH. This study investigates impedance and polarization effects in simple model electrolysis cells in order to estimate what kind of losses might be expected in such systems. A key problem is the large pH difference that develops across ion-exchange membranes that separate the anode and cathode compartments of the electrolysis cell. This pH difference, which can lead to unacceptably high efficiency losses in solar fuel modules, arises from migration of buffer ions through the membrane. Fortunately, this effect can be minimized by using high concentrations of buffers that are uncharged in either their acidic or basic form. In this case, diffusion of neutral molecules across the membrane diminishes the pH gradient created by electromigration. The results of the study suggest that with appropriate membrane materials, buffers, and cell designs, it should be possible to engineer solar fuel modules that operate efficiently.

electrical power to a polymer electrolyte membrane (PEM) or alkaline electrolyzer, where water electrolysis takes place.[2–5] Because the PV and electrolyzer modules are physically separated, there are few constraints on the design of the electrolyzer. Thus, strongly alkaline or acidic electrolytes can be used, the electrolyzer and PV module temperatures can be different, the electrolyzer current density does not need to match that of the solar cell, and light management in the electrolyzer is not an issue.

An alternative way of achieving water electrolysis is by means of a photoelectrochemical cell (PEC). In PECs, as first demonstrated by Fujishima and Honda,[6] photogenerated electrons or holes drive an electrolysis reaction at the interface of an illuminated semiconductor and an electrolyte. In the Fujishima–Honda cell, the reaction was water splitting (reactions (1)–(3)), but other electrolytic processes, such as the conversion of CO_2 to liquid fuels and oxygen, are possible. In all such reaction schemes, protons are generated at the anode and are consumed at the cathode.[7] Because a PEC integrates the functions of a solar cell and an electrolyzer, it must manage proton transport from the anode to the cathode within the material constraints of the semiconductor and other components of the cell.

$$\text{Anode: } 2H_2O_{(l)} \rightarrow O_{2(g)} + 4H^+ + 4e^-,\ 1.23\ \text{V } \textit{vs.}\ \text{NHE} \quad (1)$$

$$\text{Cathode: } 4H^+ + 4e^- \rightarrow 2H_{2(g)},\ 0.00\ \text{V } \textit{vs.}\ \text{NHE} \quad (2)$$

$$\text{Overall: } 2H_2O_{(l)} \rightarrow O_{2(g)} + 2H_{2(g)},\ 1.23\ \text{V } \textit{vs.}\ \text{NHE} \quad (3)$$

Water electrolysis is an uphill reaction, requiring a minimum input of 1.23 V. The efficiency of PECs decreases as the overpotential for driving the anode and cathode reaction increases. For this reason intensive research efforts have been focused on the development of catalysts, in particular for the four-electron oxygen evolution reaction (OER), reaction (1). In acidic PEM electrolyzers and some PECs, catalysts for this reaction are based on noble metal oxides, which have good stability and high activity. However, noble metals are expensive and their terrestrial abundance is low. Recently Nocera and coworkers have reported the development of catalysts based on cobalt-phosphate (Co-P_i) and nickel-borate (Ni-B_i).[8,9] These and other recently discovered catalysts that contain only abundant elements[9] are interesting because they can drive the OER at moderate overpotentials.

In contrast to the strongly acidic or strongly basic electrolytes of stand-alone electrolyzers, the Co-P_i and Ni-B_i catalysts work best at neutral to slightly basic pH (7–10). At these pH values electrolysis is more challenging, because the concentration of protons and/or hydroxide ions is negligible. Buffer salts are needed to maintain the anode and cathode pH and to carry protons from the anode to the cathode. Further, a membrane or porous separator is likely to be needed in practical PECs in order to prevent crossover of the fuel and oxygen produced, or in the case of gaseous products, to allow them to be generated and collected at pressures above 1 atm. Therefore is important to investigate the viability of operating electrolytic cells with buffer solutions and membranes. Although, the use of buffers and membranes is common in microbial fuel cell research,[10–15] their current density is much less than that of efficient PECs operated under AM 1.5 conditions (*ca.* 25 mA cm^{-2}). We report here the potential losses for electrolytic cells operated with buffers at pH values that are compatible with Co-P_i and Ni-P_i OER catalysts. We also explore the suitability of typical cation and anion exchange membranes to separate the products of electrolysis.

2. Experimental section

2.1 Membranes and buffer solutions

The membranes investigated were Neosepta CMX (cation exchange) and AMX (anion exchange) membranes purchased from Ameridia. These membranes are sold wet in 0.5 M NaCl, and were stored in the same solution. Prior to each measurement the membranes were soaked in the appropriate buffer for 1 h. The buffer solutions used were sodium acetate (0.1 M, 1.0 M, 3.5 M, at pH 4.4 and 4.7), NaH_2PO_4–K_2HPO_4 phosphate buffer (0.1 M, 1.0 M, 3.5 M, at pH 6.7 and 7.2), $K_2B_4O_7$–H_3BO_3 borate buffer (0.1 M, 0.5 M, 1.0 M, pH 9.3), and imidazole–imidazolium sulfate buffer (3.5 M, pH 7.0). All buffer solutions were prepared from commercial reagents and deionized (18.3 MΩ cm) water.

2.2 Tafel plots

Electrocatalytic $IrO_x \cdot nH_2O$ nanoparticles and films were prepared as previously described.[16,17] Briefly, a 2 mM $[Ir(OH)_6]^{2-}$ stock solution was made by dissolving 0.1 mmol K_2IrCl_6 in 50 mL aqueous NaOH at pH 12.1, heating it to 70 °C and then immediately cooling in an ice bath. The final solution had a pH of 7–8 and was diluted to the desired concentration with deionized water. Tafel plots for oxygen evolution were measured in a single-compartment three-electrode cell using $IrO_x \cdot nH_2O$ films deposited from these solutions at +1.0 V *vs.* Ag/AgCl on a 5 mm diameter glassy carbon rotating disk electrode (GC RDE). Current–voltage curves were obtained with a BAS 100B electrochemical workstation. A fresh $IrO_x \cdot nH_2O$ film was used for each set of buffer solutions (acetate, phosphate and borate) and the data were obtained at a rotation rate of 1000 rpm. Prior to each experiment, the solution resistance was measured with a clean GC RDE using the *iR* test function of the potentiostat. All potentials in the Tafel plots were corrected for a series resistance.

2.3 Polarization curves

The series resistance of buffer solutions and membranes was measured in a two-compartment four-electrode H cell (Fig. 1). The current carrying electrodes were platinum mesh electrodes connected to a PAR 173 potentiostat–galvanostat operated in galvanostatic mode. The reference Ag/AgCl electrodes (MI-409F, Microelectrodes Inc.) were connected to a DC voltmeter from which the potential drop was obtained. The membrane was held between the anode and cathode compartments of the cell by two O-rings and a clamp, and the geometrical area of the membrane was 0.38 cm^2 (the current densities reported are based on this area). Current–voltage curves were recorded by measuring the potential drop at current densities ranging from 0 to 25 mA cm^{-2} in increments of 0.5 mA cm^{-2}. Measurements for each buffer concentration–membrane combination were performed in triplicate. In each buffer solution, the membrane

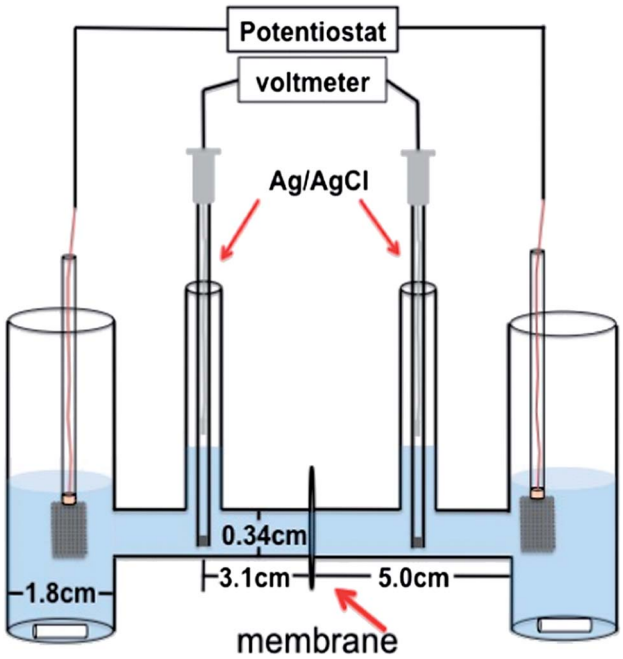

Fig. 1 Schematic of the electrolysis cell used for the polarization.

resistance was calculated as the difference between the resistances with and without the membrane in the cell.

2.4 pH gradient measurements

A smaller cell (total volume of 8 mL) was used to measure the pH gradient that developed across the membrane in hours to days of continuous electrolysis (see ESI†). The pH of each compartment was monitored with a pH electrode and the cell was operated at a current density of 25 mA cm^{-2}. A similar cell (8 mL total volume) was used to perform electrolysis in on–off mode that simulated the cycling of a photoelectrochemical cell in sunlight, where the cell was operated for 8 h at 25 mA cm^{-2} followed by 16 h off. The pH of each compartment was measured after each time period. At the moment of the pH readings, the current was turned off to avoid polarization of the electrodes. For these measurements 1.00 L stock solutions were made by mixing the buffering species in a 1 : 1 ratio to ensure that the pH = pK_a. Both the constant and the on–off electrolysis measurements were performed in triplicate. When acetate was used as the buffer, acid–base titrations were performed to estimate the fraction of buffer that was decomposed by electrolysis.

2.5 Transmembrane diffusion experiments at zero current

To determine the diffusion flux of the different buffer species, experiments were done in which one compartment contained only the acidic form of the buffer, while the other contained the basic form. An AMX membrane was used for the sodium acetate–acetic acid and phosphate diffusion experiments, whereas a CMX membrane was employed for the imidazole–imidazolium diffusion experiments. To obtain an imidazolium sulfate solution, concentrated sulfuric acid was added to an imidazole solution. In all diffusion experiments the concentration of each solution was 3.5 M and the volume of each compartment was 10 mL. The diffusion experiments were performed under stirring and purging for 24 h, with no applied current. The pH of each compartment was measured before and after this time period, and the number of moles of acid and conjugate base in each compartment was calculated using the Henderson–Hasselbach equation.

3. Results and discussion

The efficiency of any electrolytic system can be expressed, in the simplest form, as the thermodynamic potential of the electrolysis reaction divided by the operating potential. The operating potential for practical alkaline and PEM electrolyzers is in the range of 1.7–1.9 V.[3,18] This corresponds to an efficiency of 65–72%. Therefore, any PEC operated with buffer solutions should perform in this range to be competitive with PV-electrolyzer systems. A challenge in a water-splitting PEC – which is often not mentioned in studies of photoelectrodes performed in three-electrode cells – is to minimize the potential loss associated with electrolysis. This loss can be represented by the sum of the series losses in the system, as expressed in eqn (4).

$$E = \eta_{anode} + \eta_{cathode} + iR_{sol} + E_M + E_{pH} \quad (4)$$

Here the first two terms represent the anode and cathode overpotentials, the second two are the series resistance of the solution and the membrane, and the last term is the loss associated with a membrane pH gradient.

3.1 Overpotential, η

The electrode overpotentials in water splitting cells are typically dominated by the OER reaction at the anode. In order to estimate a best-case value for this overpotential at the current density of a water-splitting PEC, we measured Tafel curves of thin films of uncapped $IrO_x \cdot nH_2O$ nanoparticles. Recent studies by Murray *et al.* and by our group have shown that these films are highly active for the OER over a wide range of pH values.[16,17,19,20] Table 1 lists η values for the OER at $IrO_x \cdot nH_2O$ films ($\Gamma = 1.2 \times 10^{-7}$ mol cm^{-2}) determined from Tafel plots (see ESI†) in phosphate, borate, and acetate buffers at a current density of 25 mA cm^{-2}. The general trend, which is typical of electrolyzer catalysts operated at high current density, is that the overpotential decreases with increasing pH.[3,17,18] For cells operated under slightly alkaline solutions (pH 8.2–9.3), the OER overpotential is on the order of 200–300 mV. Allowing

Table 1 Overpotential values for water oxidation at $IrO_x \cdot nH_2O$-modified GC electrodes in buffer solutions at a current density of 25 mA cm^{-2} ($\Gamma = 1.2 \times 10^{-7}$ mol cm^{-2})

Buffer solution	η (mV)
0.1 M acetate pH 4.7	594
1.0 M acetate pH 4.7	602
3.5 M acetate pH 4.7	356
0.1 M phosphate pH 8.2	301
1.0 M phosphate pH 8.2	260
3.5 M phosphate pH 8.2	271
0.1 M borate pH 9.3	289
1.0 M borate pH 9.3	176

50–100 mV for $\eta_{cathode}$, the total overpotential contribution to eqn (4) is thus on the order of 250–400 mV. This implies that the losses from the remaining terms in eqn (4) must be kept below ~100 mV in order to have an efficient water-splitting PEC.

3.2 Solution resistance and iR_{sol}

The third term in eqn (4), iR_{sol}, is associated with the potential losses due to the resistance of the solution. Acetate, phosphate, and borate buffers were chosen because their pK_a's cover the slightly acidic, neutral, and slightly basic range. The phosphate and borate buffers are of particular interest as components of the Co-P_i and Ni-B_i catalysts. The resistance of the buffer solutions was determined from the slope of i–V curves (Fig. 2). Since the resistance of the buffers is dependent on the cell dimensions, the values are reported as conductivity, σ (see ESI†). Fig. 3 shows that the conductivities of the three buffers are similar at low concentration, whereas a significant difference (up to a factor of 4) is observed at higher buffer concentrations. Each buffer solution follows the Kohlrausch law, with conductivity proportional to the square root of the salt concentration.[21] In this regard, the conductivity is limited by the solubility of the buffer at the pH (= pK_a) where it buffers most effectively and the concentrations of the acidic and basic forms are equal. In the case of phosphate buffer, the highest concentration (3.5 M) can be achieved by using a combination of the NaH_2PO_4 and K_2HPO_4 salts, which have similar solubility to each other. For the borate buffer, the highest practical concentration was 0.9 M, which is the solubility of boric acid. Although more concentrated borate solutions can be made, the pH of the anode becomes more acidic as the electrolysis proceeds, as explained below, resulting in precipitation of boric acid crystals. In contrast, the acetate buffer can be made at a concentration as high as 17 M if CH_3COOK is used instead of the sodium salt. Based on the conductivity data, one can determine the contribution of R_{sol} to the potential loss. Since the resistance depends on the cell dimensions, we consider a PEC operating at a current density of 25 mA cm^{-2} with a 1 mm separation between the anode and cathode. For such a cell with 3.5 M phosphate buffer, the value of iR_{sol} is 16 mV. The value of iR_{sol} increases linearly with the solution path length, underscoring the need for a small anode–cathode separation distance and thus the need for a membrane or separator to allow the electrolysis products to be collected separately.

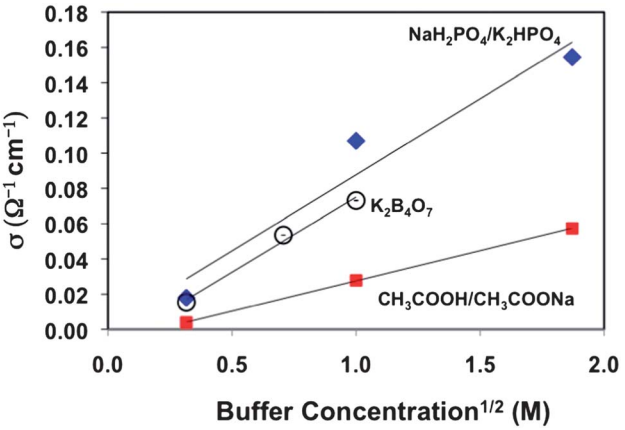

Fig. 3 Solution conductivity as a function of the square root of concentration.

3.3 Membrane resistance and E_M

Two commercial ionomer membranes were studied, a cation exchange membrane (CMX) containing strongly acidic sulfonic acid groups, and an anion exchange membrane (AMX) containing quaternary ammonium groups.[22] These membranes were stable after prolonged electrolysis. Fig. 4 illustrates the resistance values measured for these membranes in the different buffer solutions. The resistance values are in agreement with the values provided by the supplier,[22] and with those reported in the literature for similar ion exchange membranes under comparable conditions.[12] For buffer concentrations of 1 M and above, the membrane resistance is very similar for both types of membranes, and does not vary significantly as a function of pH. Conversion of the resistance values to conductivity shows that the membrane conductivities are in the same range as those measured for the 0.1 M buffer solutions (~0.01 Ω^{-1} cm^{-1}). Because the membranes are thin (200 μm), the loss associated with their series resistance is low at high buffer concentration. For example, in a 3.5 M phosphate electrolyte at 25 mA cm^{-2}

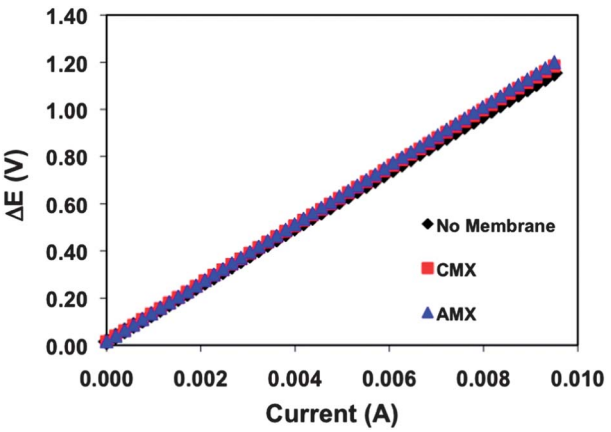

Fig. 2 Polarization curve for 1.0 M phosphate buffer pH 8.2 with and without anion- and cation-exchange membranes in the cell.

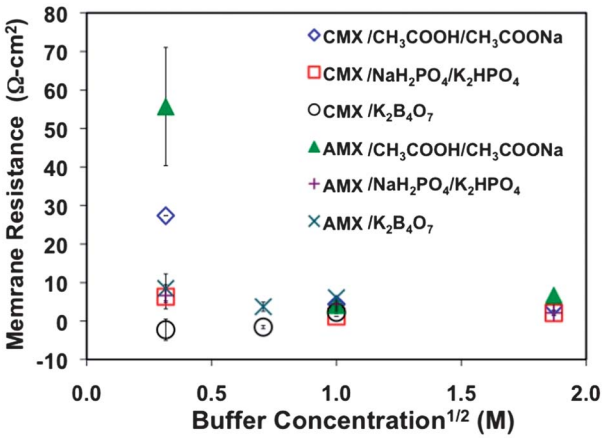

Fig. 4 CMX and AMX membrane resistance in different buffers as a function of buffer concentration.

current density, E_M (= iR_M) is 65 mV. R_M can be reduced by using thinner membranes, which in turn would reduce E_M.

3.4 pH gradient and E_{pH}

The last term in eqn (4), E_{pH}, is the potential loss due to the formation of a pH gradient across the membrane. This loss can be expressed as eqn (5),[15] where every pH unit difference corresponds to a loss of 59 mV. When water splitting is carried out under strongly acidic or basic conditions, E_{pH} is close to 0 mV.

$$E_{pH} = \frac{RT}{F}\ln\left(10^{pH_{cathode} - pH_{anode}}\right) \quad (5)$$

This can be explained by a balance sheet analysis (see ESI†),[7] as illustrated in Fig. 5A and B. Under strongly acidic or basic conditions the current is carried by protons or hydroxide ions. The mobile ion is generated at one electrode and consumed at the other, and the appropriate ion exchange membrane (which typically contain sulfonate or quaternary ammonium groups for acid or base electrolysis, respectively), is completely charge-compensated by the mobile ion. Under these conditions the balance sheet is very simple. The current is carried entirely by migration of the mobile H^+ or OH^- ion, which is present everywhere in high concentration, so no proton gradient is created.

In contrast, in an electrolysis cell near neutral pH, the H^+ and OH^- concentrations are orders of magnitude lower than the concentration of the buffer salts, both in the solution and in the membrane. Thus, their contribution to the ion current is negligible. To measure E_{pH}, the buffer-based electrolytic cell was operated at 25 mA cm^{-2} while monitoring the pH of the cathode and anode compartments.

When a non-buffering salt, such as $NaNO_3$, was used, as expected a substantial pH gradient was formed within 10 min., even at high salt concentration (Table 2). Fig. 6a shows that the pH gradient develops more slowly when buffer solutions are used, especially concentrated buffers. Over the course of 6.5 h, a pH gradient of ~6 pH units (E_{pH} = 341 mV) develops across the AMX anion exchange membrane with 1.0 M phosphate buffer. If the concentration of the buffer is increased, the development of the pH gradient is significantly delayed but eventually occurs.

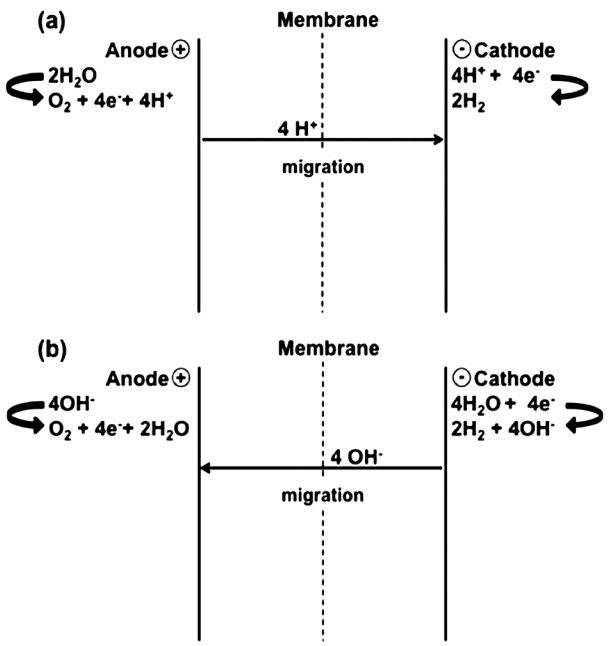

Fig. 5 Balance sheets for electrolysis in strong (a) acid and (b) base.

A balance sheet analysis of migration and diffusion in the phosphate buffer solution–AMX cell is shown in Fig. 7a. Because the AMX membrane is an anion exchanger, the concentration of cations (K^+ and Na^+) in the membrane is quite low and to a first approximation they can be considered to carry no current. Thus the migration current is carried entirely by HPO_4^{2-} and $H_2PO_4^-$ anions. These ions migrate from the cathode to the anode, depleting the buffer in the cathode compartment and causing a sharp increase in pH there (Fig. 6a). A titration analysis of the cathode compartment after 24 h electrolysis with 3.5 M phosphate buffer confirms that phosphate is depleted on that side of the cell (see ESI†). When 8.5 meq. of charge was passed in the cell, 7.6 mmol phosphate migrated through the AMX membrane. This result indicates most of the migration current is carried by $H_2PO_4^-$ and a smaller fraction (~25%) is carried by HPO_4^{2-}. The pH change is less dramatic in the anode compartment because buffer ions migrate to that side of the cell.

Fig. 6b compares the polarization of AMX and CMX membranes with 3.5 M phosphate buffer. CMX is a cation exchanger, so the current is carried by migration of K^+ and Na^+ ions from the anode to the cathode. Since the phosphate anions cannot migrate across the membrane, this results in a decrease of the pH on the anode side as seen in Fig. 6b. In this case, the pH change is more symmetric because buffer anions do not cross the membrane. Table 2 shows that a large pH gradient also develops across an AMX membrane after 18 h of electrolysis using an acetate buffer. In this system the current is carried by the OAc^- anion. As in the phosphate system, the buffer is depleted in the cathode compartment as the electrolysis proceeds (Fig. 6b).

In these experiments the electrolysis was run continuously for 18–24 h, which is quite different from the operation of an actual photoelectrochemical cell. In order to simulate the diurnal cycle of an efficient photoelectrochemical cell, electrolysis was cycled between 8 h at 25 mA cm^{-2} and 16 h at zero current. The results of these experiments, comparing phosphate and acetate buffers with the AMX anion exchange membrane, are shown in Fig. 8. Again, the largest pH excursion is on the cathode side of the cell because the buffer anions are driven by migration from the cathode to the anode, and in the case of phosphate a precipitate forms in the anode compartment. For both phosphate and acetate buffers, the "on" cycles increase the pH gradient while the "off" cycles lead to a recovery or depolarization. However a marked difference can be seen in the third cycle. In the third "on" cycle the pH gradient increases for both buffers, but for the acetate buffer E_{pH} is a factor of ~2 higher than for phosphate. However, after the "off" cycle a dramatic difference is observed in the recovery of the two systems. E_{pH} is reduced by 118 mV for the phosphate buffer, while that of acetate is reduced by 421 mV.

The diffusion of neutral and charged ions through the membrane, which is responsible for membrane depolarization at zero current, is illustrated schematically in Fig. 9. In the case of

Table 2 E_{pH} for various buffer and membrane combinations

Buffer	Membrane	Time (h)	pH_{anode}	$pH_{cathode}$	E_{pH} (mV)
1.0 M phosphate pH 6.73	AMX	6.5	5.55 ± 0.05	11.30 ± 0.03	341 ± 21
3.5 M phosphate pH 6.72	AMX	24	5.91 ± 0.06	11.33 ± 0.03	320 ± 26
3.5 M phosphate pH 6.72	CMX	24	2.22 ± 0.07	11.27 ± 0.03	535 ± 19
3.5 M acetate pH 4.39	AMX	18	4.27 ± 0.06	12.50 ± 0.30	489 ± 77
3.5 M $NaNO_3$	CMX	0.17	1.30 ± 0.20	11.60 ± 0.20	611 ± 63

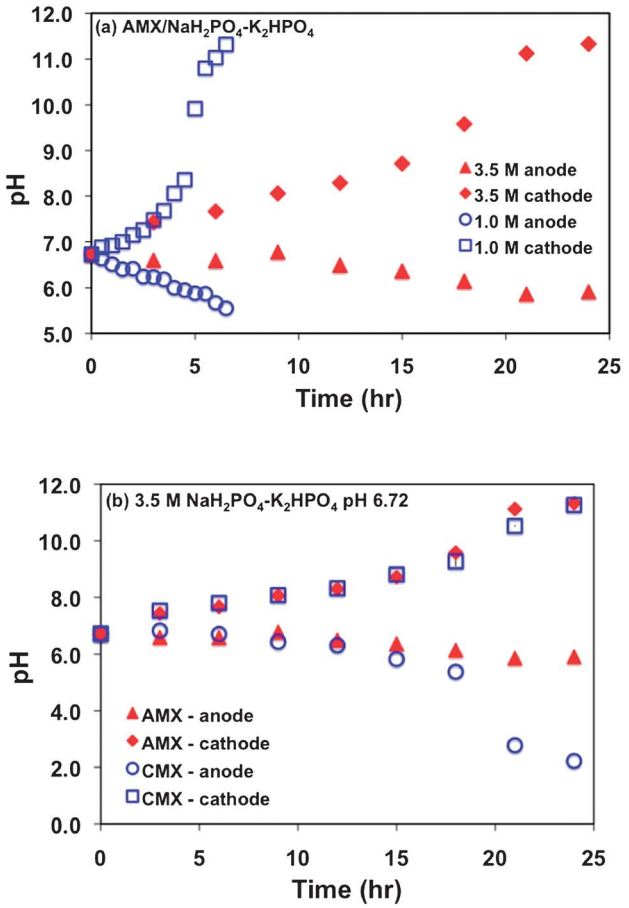

Fig. 6 pH gradient formation in electrolysis cells with (a) AMX membranes and 1.0 and 3.5 M phosphate buffers (initial pH 6.72). (b) 3.5 M phosphate buffer with AMX (red) and CMX (blue) membranes.

the phosphate buffer (Fig. 9a), depolarization of the anion exchange membrane cannot occur by simple diffusion of acidic $H_2PO_4^-$ ions from the anode to the cathode side because that process would be electrogenic. Three other possible non-electrogenic processes are diffusion of neutral H_3PO_4, which is present in appreciable quantities below pH ~4, diffusion of $Na^+H_2PO_4^-$ ion pairs, and simultaneous diffusion of $2H_2PO_4^-$ and HPO_4^{2-} in opposite directions. In the case of the acetate buffer (Fig. 9b), the AMX membrane is depolarized by diffusion of neutral acetic acid molecules from the anode to the cathode. With the CMX cation exchange membrane, a similar depolarization process can occur by diffusion of a neutral base (shown as imidazole in Fig. 9c) from the cathode to the anode side of the membrane.

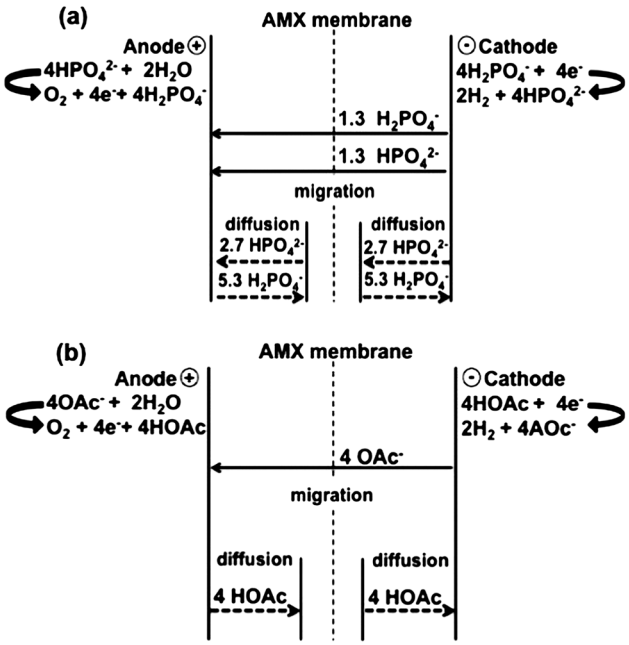

Fig. 7 Balance sheets for electrolysis in (a) phosphate buffer, and (b) acetate buffer.

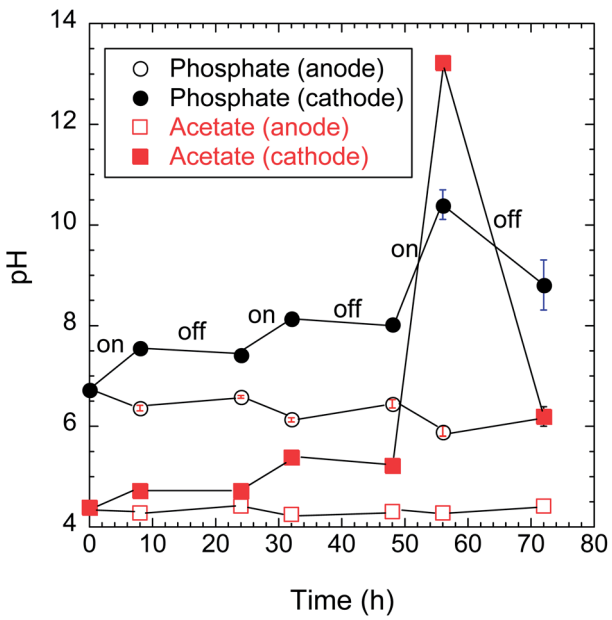

Fig. 8 Anode and cathode pH changes induced in three electrolysis cycles of 8 h on (25 mA cm^{-2})/16 h off, for 3.5 M phosphate–AMX and 3.5 M acetate–AMX.

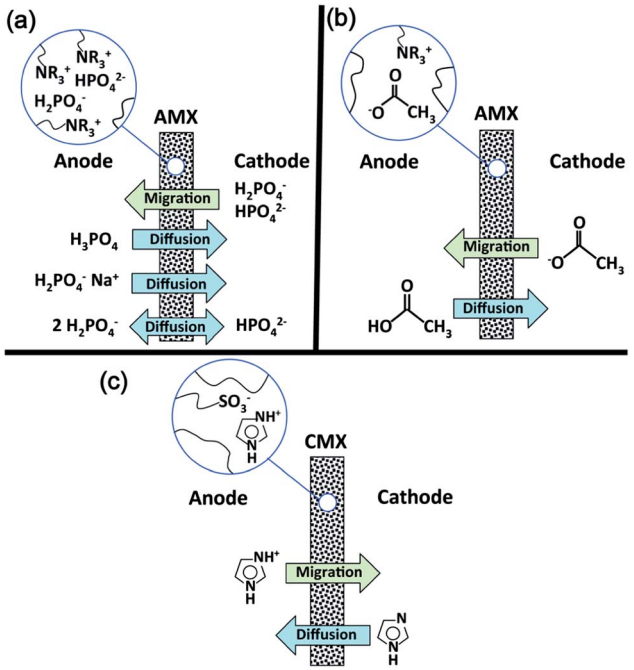

Fig. 9 Schematic illustration of buffer transport by migration and diffusion for (a) phosphate–AMX membrane (b) acetate–AMX membrane and (c) imidazole–CMX membrane.

The relative rates of diffusion were measured in a membrane cell at zero current, placing 3.5 M solutions of the acidic and basic form of the buffer on each side. The results of these experiments are shown in Table 3 for acetate and phosphate buffers, using AMX membranes, and for imidazole–imidazolium (ImH^+) using CMX. From the pH changes on the two sides of the membrane, the final concentration of each species could be calculated, and from these concentrations the diffusional flux J_D of each species was obtained (see ESI†).

The results of these diffusion experiments show that at low pH (*i.e.*, in solutions of $Na^+H_2PO_4^-$ near pH 4) the diffusion flux is dominated by neutral H_3PO_4 and there is relatively little contribution from $Na^+H_2PO_4^-$ ion pairs. The diffusion of $H_2PO_4^-$ and HPO_4^{2-} anions in opposite directions cannot be distinguished in this experiment from the diffusion of H_3PO_4 because the net change in composition is the same. Since the first mechanism is unavailable near neutral pH where the concentration of H_3PO_4 is very low, the depolarization of the AMX membrane is slower using phosphate buffer (Table 3); this result, from on–off cycling of the cell, indicates that counter-diffusion of $H_2PO_4^-$ and HPO_4^{2-} anions does not occur rapidly on the timescale of 16 h.

Table 3 pH changes and diffusion fluxes (J_D) for acetate and phosphate buffers (AMX membrane) and imidazole buffer (CMX membrane)

Solution	Initial conc. (M)	Initial pH	pH after 24 h	ΔC (M)	J_D (mol cm^{-2} s)
Na^+OAc^-	3.5	8.22	6.17	3.6×10^{-2}	1.1×10^{-8}
HOAc	3.5	1.84	2.76	1.3×10^{-1}	4.0×10^{-8}
$Na^+H_2PO_4^-$	3.5	3.55	4.12	4.5×10^{-2}	1.3×10^{-8}[a]
$(K^+)_2HPO_4^{2-}$	3.5	9.83	8.49	4.5×10^{-2}	1.3×10^{-8}[a]
Imidazole	3.5	10.38	9.79	1.6×10^{-1}	4.8×10^{-8}
$(ImH^+)_2SO_4^{2-}$	3.5	3.45	5.67	4.2×10^{-3}	1.3×10^{-9}

[a] Represents primarily the flux of neutral H_3PO_4.

Neutral imidazole and neutral acetic acid have comparable fluxes through CMX and AMX membranes, respectively, and the diffusional flux of their conjugates (as ion pairs) is much smaller. In order for E_{pH} to remain constant under steady-state conditions of water photoelectrolysis, the diffusion flux, J_D, of the neutral form of the buffer must be equal and opposite to the migration flux, J_M, of the charged form. A current density of 25 mA cm^{-2} corresponds to $J_M = 2.6 \times 10^{-7}$ mol cm^{-2} s, which is ~6 times larger than the largest J_D values shown in Table 3. This is consistent with the polarization of the AMX membrane with both acetate and phosphate buffers, and with the depolarization found with acetate buffer after 16 h of passing zero current (Fig. 8). The diffusion flux J_D should be inversely proportional to the thickness of the membrane. It follows from this analysis that very concentrated (≥3 M) buffers such as acetate, which are uncharged in one conjugate form, should be able to maintain low E_{pH} values with membranes that are ~6 times thinner (or more permeable) than those used in this study.

Imidazole was studied as a possible candidate of a neutral base–cationic acid buffer that would also have a low E_{pH} when used with the CMX membrane. When an on–off electrolysis experiment was performed using 3.5 imidazole–imidazolium sulfate buffer the system also showed some recovery. This is consistent with the J_D value for imidazole–CMX, which is comparable to that of acetic acid–AMX (Table 3). However, during the electrolysis, oxidative polymerization of imidazole occurs in parallel with water oxidation,[23] affecting the buffer capacity. This suggests that the kind of system represented in Fig. 9c is potentially viable, but a more stable neutral base must be identified.

A similar electrolysis experiment was attempted with a 0.5 M and 1.0 M borate buffers. Based on simulation results using the MINEQL+ program (see ESI†), the predominant basic species in the borate buffer ($H_2BO_3^-$, $H_8(BO_3)_3^-$, and $H_5(BO_3)_2^-$) all carry a −1 charge, and the acidic species is neutral H_3BO_3. By analogy to the acetate case, we would expect the pH gradient developed across an AMX membrane to be mitigated by boric acid diffusion from the anode to the cathode side. However, because of its low solubility, boric acid precipitates on the anode side of the cell. For this reason, the cell could not be operated for more than a few hours.

4. Conclusions

The viability of solar fuel production in PECs is dependent on the efficiency of the electrolysis reaction, which in turn depends on series losses in the cell. When gaseous products such as hydrogen and oxygen are made, or when organic compounds are synthesized at the cathode, a membrane or separator is likely to be needed in the PEC to prevent crossover and product loss. Spurgeon and Lewis have recently demonstrated that water electrolysis can be sustained with low resistive loss in vapor-phase electrolysis cells that resemble PEM fuel cells.[24] However in those cells acidic membranes were used, and such membranes may not be compatible with catalysts such as Co-P_i and Ni-B_i, or with semiconductors that are unstable in an acidic environment.

The experiments reported here quantify the series losses that will be encountered in water-splitting PECs operated with aqueous buffer solutions and typical anion- or cation-exchange membranes. Not unexpectedly, anode polarization is a major contributor to loss at the current density of an efficient PEC operating in full sun (~25 mA cm^{-2}). Even with very active catalysts such as $IrO_x \cdot nH_2O$, the anode and cathode overpotentials together are expected to be 250–400 mV, the value depending on the pH of the cell. The loss associated with membrane series resistance is 50–100 mV at high buffer concentration, but this loss can likely be minimized with thinner membranes. The AMX and CMX membranes used in this study were 200 μm thick, but chemically similar membranes used in PEM fuel cells can be much thinner (50–100 μm), especially if they are supported in composite structures. High buffer concentration also minimizes the solution series resistance, which results in losses on the order of 160 mV for a 1 cm path length cell, or 16 mV for a 1 mm cell containing 3.5 M phosphate buffer. These simple measurements underscore the need for small liquid volumes and short path lengths in practical PEC designs.

The most problematic source of loss in buffer-based electrolysis cells is the development of a pH gradient across the membrane. This was observed even in concentrated buffer solutions (*e.g.*, 3.5 M phosphate) and leads to E_{pH} values of several hundred mV. The problem is exacerbated by migration of buffer anions across the AMX anion exchange membrane. However, this problem can be largely mitigated with both anion- and cation-exchange membranes by back diffusion of neutral acids and bases, respectively. Although more detailed studies of membrane permeability will be needed in order to design more efficient membrane–buffer combinations, the preliminary results obtained with acetate–acetic acid–AMX and imidazolium–imidazole–CMX are encouraging. A drawback of the imidazole system is the oxidative instability of the base, and more stable buffers must be found for use with cation exchange membranes. Again, thinner membranes should result in faster diffusion of the neutral acid or base across the membrane, resulting smaller steady-state pH gradients and lower loss associated with E_{pH}.

Finally, it is important to note that we have studied only anion and cation exchanger membranes that have no intrinsic buffer capacity and are designed for use in strongly acidic or basic media. Weak acid membranes and bipolar polymer membranes[25] could potentially offer some advantages and should be studied in the context of photoelectrolysis of solutions near neutral pH.

Acknowledgements

This work was supported by the Office of Basic Energy Sciences, Division of Chemical Sciences, Geosciences, and Energy Biosciences, U.S. Department of Energy under contract DE-FG02-07ER15911.

Notes and references

1 N. S. Lewis and D. G. Nocera, *Proc. Natl. Acad. Sci. U. S. A.*, 2006, **103**, 15729.
2 A. Dukic and M. Firak, *Int. J. Hydrogen Energy*, 2011, **36**, 7799.
3 K. Zeng and D. K. Zhang, *Prog. Energy Combust. Sci.*, 2010, **36**, 307.
4 A. Djafour, M. Matoug, H. Bouras, B. Bouchekima, M. S. Aida and B. Azoui, *Int. J. Hydrogen Energy*, 2011, **36**, 4117.
5 T. L. Gibson and N. A. Kelly, *Int. J. Hydrogen Energy*, 2008, **33**, 5931.
6 A. Fujishima and K. Honda, *Nature*, 1972, **238**, 37.
7 A. J. Bard and L. R. Faulkner, *Electrochemical Methods: Fundamentals and Applications*, Wiley, New York, 2001.
8 M. Dinca, Y. Surendranath and D. G. Nocera, *Proc. Natl. Acad. Sci. U. S. A.*, 2010, **107**, 10337.
9 A. J. Esswein, Y. Surendranath, S. Y. Reece and D. G. Nocera, *Energy Environ. Sci.*, 2011, **4**, 499.
10 Y. Z. Fan, H. Q. Hu and H. Liu, *Environ. Sci. Technol.*, 2007, **41**, 8154.
11 Y. Z. Fan, E. Sharbrough and H. Liu, *Environ. Sci. Technol.*, 2008, **42**, 8101.
12 F. Harnisch, U. Schroder and F. Scholz, *Environ. Sci. Technol.*, 2008, **42**, 1740.
13 J. Y. Nam, H. W. Kim, K. H. Lim, H. S. Shin and B. E. Logan, *Biosens. Bioelectron.*, 2010, **25**, 1155.
14 R. A. Rozendal, H. V. M. Hamelers and C. J. N. Buisman, *Environ. Sci. Technol.*, 2006, **40**, 5206.
15 T. H. J. A. Sleutels, H. V. M. Hamelers, R. A. Rozendal and C. J. N. Buisman, *Int. J. Hydrogen Energy*, 2009, **34**, 3612.
16 T. E. Mallouk, Y. X. Zhao, E. A. Hernandez-Pagan, N. M. Vargas-Barbosa and J. L. Dysart, *J. Phys. Chem. Lett.*, 2011, **2**, 402.
17 Y. Zhao, N. M. Vargas-Barbosa, E. A. Hernandez-Pagan and T. E. Mallouk, *Small*, 2011, **7**, 2087.
18 V. M. Nikolic, G. S. Tasic, A. D. Maksic, D. P. Saponjic, S. M. Miulovic and M. P. M. Kaninski, *Int. J. Hydrogen Energy*, 2010, **35**, 12369.
19 T. Nakagawa, C. A. Beasley and R. W. Murray, *J. Phys. Chem. C*, 2009, **113**, 12958.
20 T. Nakagawa, N. S. Bjorge and R. W. Murray, *J. Am. Chem. Soc.*, 2009, **131**, 15578.
21 J. O. M. Bockris and A. K. N. Reddy, *Modern Electrochemistry 1: Ionics*, Plenum Press, New York, 1998.
22 *NEOSEPTA ion exchange membranes*, Product brochure Tokuyama Soda Inc.
23 H. L. Wang, R. M. Omalley and J. E. Fernandez, *Macromolecules*, 1994, **27**, 893.
24 J. M. Spurgeon and N. S. Lewis, *Energy Environ. Sci.*, 2011, **4**, 2993.
25 M. Ünlü, J. Zhou and P. A. Kohl, *J. Phys. Chem. C*, 2009, **113**, 11416.